

The turbulent convection in protoplanetary disks and its role in the angular momentum transfer

E. P. Kurbatov^{1*} and Ya. N. Pavlyuchenkov^{1†}

¹*Institute of Astronomy of the RAS, Moscow, Russia*

Accepted XXX. Received YYY; in original form ZZZ

ABSTRACT

A model for the transport of anisotropic turbulence in an accretion disk is presented. This model is based on the mean field approximation and is designed to study turbulence of various nature and its role in the redistribution of the angular momentum of the accretion disk. The mean field approach makes it possible to take into account various types of instabilities by adding appropriate sources in the form of moments of fluctuations of hydrodynamic quantities. We used the model to study the role of convective instability in a gaseous and dusty circumstellar disk in the framework of a one-dimensional approximation. To do this, it was combined with the calculation of radiative transfer and with the calculation of the convective flow in the mixing length theory approximation. Within this framework, we confirm the conclusions of other authors that the turbulence generated by convection does not provide the observable disk accretion rates and sufficient heat source for which convection would be self-sustaining. The reasons for this are the strong anisotropy of turbulence in the disk, as well as the fact that convection turns out to be too weak source for turbulence.

Key words: accretion, accretion disks – protoplanetary discs – convection – instabilities – turbulence

1 INTRODUCTION

The theory of disk accretion is used in astrophysics to explain a wide range of observed sources and phenomena: active galactic nuclei, the evolution and variability of close binary systems, the formation of jets and bipolar outflows, the structure of protoplanetary disks, the formation of planetary systems, and many others, see for example [Shakura \(2018\)](#); [Hartmann \(2009\)](#); [Armitage \(2015\)](#). In all these objects, accretion proceeds under various physical conditions, which differ in temperature, density, degree of ionization, magnetic induction, radiation field, presence of dust, etc. However, the processes that affect accretion have common consequences: this is the redistribution and removal of angular momentum, providing accretion of matter from the disk to the central object.

It is believed that in many cases turbulence plays an important role in providing accretion. The classical approach to describe accretion caused by turbulence uses the formalism of turbulent viscosity, which is mathematically equivalent to molecular viscosity. Within the framework of the [Shakura & Sunyaev \(1973\)](#) model, this formalism is reduced to setting an alpha parameter, which relates the coefficient

of turbulent viscosity to the speed of sound and the height of the disk. This phenomenological approach turned out to be extremely useful for describing the structure and evolution of astrophysical disks, but the question of the causes and properties of turbulence itself remains beyond its scope.

One of the most actively studied astrophysical objects at present is protoplanetary disks around young stars. This interest is associated with progress in observational techniques and with the possibility of obtaining direct images of disks at various wavelengths, see review [Andrews \(2020\)](#). The high angular and spectral resolution makes it possible to reconstruct, among other things, the detailed distribution of the turbulent gas velocity over the disk, the intensity estimates of which vary greatly for different sources, see [Flaherty et al. \(2017\)](#); [Guilloteau et al. \(2012\)](#). In this regard, protoplanetary disks can be considered as convenient natural laboratory for studying the physics of accretion and turbulence in general.

It is generally accepted that the cause of turbulence is some kind of instability. In protoplanetary disks, the possible triggers of turbulence could be gravitational, thermal, magneto-rotational, baroclinic, streaming, shear, and other instabilities (see the reviews [Armitage \(2015\)](#); [Bae et al. \(2022\)](#) and [Lesur et al. \(2022\)](#)). Each possible instability is a subject of deep research. For instance, in [Klahr & Hubbard \(2014\)](#), the authors considered the effects of buoyancy

* E-mail: kurbatov@inasan.ru

† E-mail: pavlyar@inasan.ru

in disks in the radial direction. It was shown that in a rotating flow, radial buoyancy, together with centrifugal force, can cause epicyclic oscillations with increasing amplitude. This phenomenon has been called convective overstability. In the non-linear regime, this instability can generate a sub-critical baroclinic instability (Lyra 2014), as well as lead to the growth of large-scale vortices, which, presumably, can play their role in planet formation (Raettig et al. 2021).

In the presented work, our interest is connected with convective instability in the vertical direction. The binding of convection, turbulence and the redistribution of angular momentum has been studied in many studies. The idea that convection in protoplanetary disks can not only transfer heat, but also provide viscosity and thus influence disk evolution, was formulated in Cameron (1978) and Lin & Papaloizou (1980). This caused great enthusiasm, but after several decades of research, the role of convection in the transfer of angular momentum is still debatable, see a detailed historical review in Klahr (2006). An indicative example is that in early numerical models it turned out that convection causes the transfer of angular momentum towards the accretor (Stone & Balbus 1996), which would correspond to a negative alpha parameter. In later works, using exact numerical schemes, it was shown that in reality the angular momentum of the accreting matter is transferred outward, in full accordance with theoretical concepts (see the paper of Held & Latter (2021) and the discussion therein).

With the availability of high-quality images of protoplanetary disks and the observation of ring structures in them, interest in hydrodynamic models of convection has increased again. In particular, Held & Latter (2018) presents the results of 3D modeling of convection in a disk, which illustrates the emergence of convective cells, vortices, and other coherent structures upon initiation of convection. At the same time, the authors of Held & Latter (2018) note that they fail to obtain a self-sustaining convection regime in the disk. In Held & Latter (2021) it is demonstrated that the interaction of convective and magneto-rotational instabilities ensures the periodic character of accretion in the disk. Pavlyuchenkov et al. (2020) and Maksimova et al. (2020) also show that convective instability in a protoplanetary disk can lead to irregular accretion onto a star. This result is relevant in connection with the search for physical mechanisms to confirm the scenario of episodic accretion in protoplanetary disks (Hartmann 2009), which is important for solving the problem of observed accretion luminosities and explaining the nature of young flaring objects such as FU Ori and EX Lupi. However, the key approximation of the model presented in Pavlyuchenkov et al. (2020) is the assumption that the emerging convection is accompanied by high turbulent viscosity.

A picture of the relationship between convection, turbulence and accretion in the disk layer can be presented in Fig. 1, which is based on the energy circulation scheme. Let there be some initial source leading to heating of the medium. Thermal energy is transferred and ultimately emitted by diffusion of infrared radiation. Under certain conditions, convection can also occur, which not only transfers part of the heat, but also excites turbulence. Dissipation of turbulence eventually returns kinetic energy to thermal energy. In addition to this cycle, it must also be taken into account that the background shear flow can enhance tur-

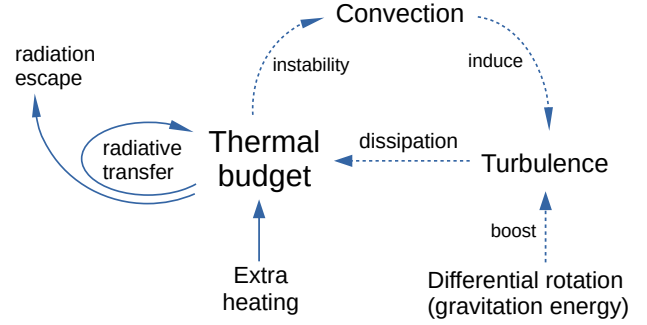


Figure 1. Energy circulation in an accretion disk with a convective source of turbulence.

bulence, the kinetic energy of which, as a result of dissipation, will replenish the heat budget, also acting as an energy source for convection. Thus, turbulence will additionally transfer the gravitational energy of the gas into thermal energy. The fundamental question in this picture is how significant the increase in turbulence will be due to the transfer of energy from the differential rotation of the disk.

Despite the fact that direct numerical simulation can give the picture closest to reality, a complete self-consistent three-dimensional calculation of the evolution of the accretion disk with a sufficiently high space-time resolution is still a difficult task. In our opinion, to study the problem of turbulent convection and its role in the redistribution of angular momentum, one can use a simpler for calculations, but effective approach to describing the accretion flow, based on the mean field model. In this paper, we attempted to develop the accretion disk model towards a more realistic description of the physical conditions. We implement a non-isotropic turbulence transport model (in the mean field approximation), along with a calculation of the convective flow (in the mixing length approximation) and carefully account for radiative transport.

In the next section, a brief derivation of the equations of mean flow hydrodynamics and turbulence transfer equations, as well as a method for closing the system of equations, is given. In the third section, the implementation of the turbulent convection model in the framework of the one-dimensional approximation is considered and an example of calculating the structure of a vertical column in a protoplanetary disk is given. Discussion and conclusion are given in the last section.

2 MODEL OF CONVECTION-GENERATED TURBULENCE IN A CIRCUMSTELLAR DISK

2.1 Mean field and turbulence transfer equations

As noted in the introduction, the mean field approach will be used to model turbulence. Within the framework of this approximation, two methods of description can be distinguished: the filtering method and the statistical method. The first uses a spatial and temporal filter with some given scales. Details of the sub-scale flow are taken into account only approximately as averages on the filter scale. This approach is implemented in the class of subgrid models and

in the Large Eddy Simulation (LES, Leonard (1975); Meneveau et al. (1996)). Another method is that turbulent fluctuations are assumed to be stochastic, a statistical ensemble is introduced for them, and the properties of the fluctuation field are formulated in terms of the statistical moments of this ensemble (see e.g. references in Canuto (1997)). Since in any particular problem there is only one realization of the flow, the LES method may seem to be more physically justified. In addition, this method can explicitly describe non-local manifestations of turbulence, such as the interaction of structures of different scales and near-wall effects (Leonard 1975; Stewart 1976). The statistical approach, in turn, makes it possible to significantly simplify calculations, since it makes it possible to use empirical information about fluctuation amplitudes, their correlation, and other parameters. Therefore, to describe the dynamics of a turbulent flow, we will use the statistical approach in the mean field approximation. We will not be interested in the detailed spatial and temporal structure of turbulence, but only in its influence on the mean flow, therefore, to describe the properties of turbulence, we will use the statistical moments of velocity, density, and pressure fluctuations.

We will not give detailed calculations of the turbulence transfer model, but will only borrow the derivation scheme from Canuto (1992, 1997) (see also references therein), where the problem of turbulent convection in a stratified atmosphere is considered. We will proceed from the hydrodynamic equations written in arbitrary curvilinear coordinates:

$$\frac{\partial \rho}{\partial t} + \nabla_k(\rho v^k) = 0, \quad (1)$$

$$\frac{\partial(\rho v^i)}{\partial t} + \nabla_k(\rho v^i v^k) = -\nabla^i p + \nabla_k \sigma^{ik} + f^i, \quad (2)$$

$$\frac{\partial(\rho e)}{\partial t} + \nabla_k[(\rho e + p) v^k] = v^k \nabla_k p + \sigma^{jk} \nabla_k v_j + q. \quad (3)$$

Here ρ and v^i are the density and mass velocity of the gas; p is the gas pressure; e is the internal energy of gas per one particle; σ^{ik} is the microscopic viscous stress tensor; f^i is the volumetric density of external forces (gravity, electromagnetic forces); q is the external source of thermal energy, in the context of astrophysical disks, it can be associated with radiation and dust; ∇_i is the operator of covariant spatial derivative. We supplement the system of equations (1)–(3) with the thermodynamic equation of state for an ideal gas:

$$p = \frac{\mathcal{R}}{\mu} \rho T, \quad e = C_v T, \quad (4)$$

$$C_p = \frac{\gamma}{\gamma - 1} \frac{\mathcal{R}}{\mu}, \quad C_v = \frac{1}{\gamma - 1} \frac{\mathcal{R}}{\mu}, \quad (5)$$

where μ is the weight of a gas particle in hydrogen atom mass units, m_H ; $\mathcal{R} = k_B/m_H = 8.25 \times 10^7 \text{ erg g}^{-1} \text{ K}^{-1}$ is the gas constant; γ is the adiabatic index.

We introduce a linear operator $\langle \cdot \rangle$, which averages over an ensemble of turbulent flow samples. The ensemble mean will be denoted by a bar above. The averaging rules are different for quantities defined per unit volume (such as ρ and p) and units mass (v^i , e , T): (Canuto 1997):

$$\bar{\rho} \equiv \langle \rho \rangle, \quad \rho = \bar{\rho} + \delta \rho, \quad \langle \delta \rho \rangle = 0, \quad (6)$$

$$\bar{v}^i \equiv \langle \rho v^i \rangle / \langle \rho \rangle, \quad v^i = \bar{v}^i + \delta v^i, \quad \langle \rho \delta v^i \rangle = 0. \quad (7)$$

For other fields, averaging is written similarly. Let us apply

the averaging operator one by one to all equations of the system (1)–(3). The continuity equation does not change:

$$\frac{\partial \bar{\rho}}{\partial t} + \nabla_k(\bar{\rho} \bar{v}^k) = 0. \quad (8)$$

In the equation of motion (2), after averaging, a quadratic term $\langle \rho v^i v^k \rangle$ appears, which we write as follows:

$$\langle \rho v^i v^k \rangle = \bar{\rho} \bar{v}^i \bar{v}^k + \langle \rho \delta v^i \bar{v}^k \rangle + \langle \bar{v}^i \rho \delta v^k \rangle + \langle \rho \delta v^k \delta v^i \rangle. \quad (9)$$

Further, we will assume that the averages of linear (in fluctuations) values reduced to unit volume are always zero, which means $\langle \rho \delta v^i \bar{v}^k \rangle = \langle \bar{v}^i \rho \delta v^k \rangle = 0$. Then we can write:

$$\langle \rho v^i v^k \rangle = \bar{\rho} \bar{v}^i \bar{v}^k + w^{ik}, \quad (10)$$

$$w^{ik} = \langle \rho \delta v^i \delta v^k \rangle, \quad (11)$$

for w^{ik} is the turbulent viscous stress tensor, it bears the main information about local turbulence. The equation of motion of the medium takes form:

$$\frac{\partial(\bar{\rho} \bar{v}^i)}{\partial t} + \nabla_k(\bar{\rho} \bar{v}^i \bar{v}^k) = -\nabla^i \bar{p} - \nabla_k w^{ik} + \nabla_k \langle \sigma^{ik} \rangle + \langle f^i \rangle. \quad (12)$$

Let us pay attention to the fact that the stress tensors w^{ik} and $\langle \sigma^{ik} \rangle$ have different signs in the momentum conservation law (12).

The w^{ik} tensor is not an independent quantity; its components must be expressed in terms of mean flow characteristics. In simple models, the gradient approximation is used for this, namely, it is assumed that turbulent stresses are proportional to the gradient of the mean flow velocity, by analogy with microscopic viscosity. This can be written as follows:

$$w^{ik} = -\langle \delta v \ell \rangle [\nabla^i(\bar{\rho} \bar{v}^k) + \nabla^k(\bar{\rho} \bar{v}^i)], \quad (13)$$

where ℓ should be considered as the spatial scale of the velocity perturbation, and the average $\langle \delta v \ell \rangle$ can be called the kinematic turbulent viscosity coefficient. The difficulty with the closure (13) is that the turbulent viscosity coefficient is still undefined. In order to set it, it is necessary, at least, to know the amplitude of turbulent velocity fluctuations, as well as the characteristic scale or time of their correlation. These quantities generally depend on the coordinates and time, as well as on the mean velocity field. For astrophysical disks, the coefficient of kinematic turbulent viscosity is often expressed in terms of the speed of sound and the semi-thickness of the gaseous disk: $\alpha c_s H$, where α is the turbulence parameter (Shakura & Sunyaev 1973).

There is a class of models, the so-called “Energy-dissipation models”, in which the energy transfer of turbulent fluctuations K is described in a closed form together with one of the following quantities: the characteristic turbulence scale ℓ (model “ $K - \ell$ ”), dissipation rate (“ $K - \epsilon$ ”), reverse time dissipations (“ $K - \omega$ ”) (Launder 1974). One variant of the “ $K - \epsilon$ ” model was used to calculate the vertical structure of the accretion disk in Nakao & Kato (1994, 1995). In the models of this class, it is assumed that turbulence is locally isotropic. Indeed, a developed flow can have such a property far from the source of turbulence, which, under the conditions of a laboratory experiment, can be a channel wall or a divertor. In astrophysical disks, the source of turbulence can be convective instability, i.e. naturally anisotropic. Moreover, differential rotation in the disk can intensify the turbulence. Thus, the anisotropy of the physical conditions

will be significant over the entire volume of the disk flow. Therefore, we believe that it will be correct to calculate the transfer of the w^{ij} tensor explicitly, without resorting to an approximation of the form (13).

The equation for the turbulent stress tensor is obtained by averaging the equations for quadratic velocity fluctuations $\rho \delta v^i \delta v^k$. In the notation adopted in Canuto (1997), it has the form

$$\begin{aligned} \frac{\partial w^{ij}}{\partial t} + \nabla_k (w^{ij} \bar{v}^k + w^{ijk}) \\ = - (w^{ik} \nabla_k \bar{v}^j + w^{jk} \nabla_k \bar{v}^i) + B^{ij} - \Pi^{ij} + X^{ij}. \end{aligned} \quad (14)$$

On the right side, there are second-order correlators between the velocity, density, and pressure components. B^{ij} is called the buoyancy tensor, it arises with the advent of convection,

$$B^{ij} = - \frac{\nabla^i \bar{p}}{\rho} \bar{\rho} \langle \delta v^j \rangle - \frac{\nabla^j \bar{p}}{\rho} \bar{\rho} \langle \delta v^i \rangle. \quad (15)$$

The Π^{ij} tensor describes the exchange between turbulence components in different spatial directions,

$$\Pi^{ij} = \langle \delta v^i \nabla^j \delta p \rangle + \langle \delta v^j \nabla^i \delta p \rangle. \quad (16)$$

The tensor X^{ij} is related to the dissipation of turbulent energy,

$$X^{ij} = \nabla_k \langle \delta v^i \delta \sigma^{jk} \rangle + \nabla_k \langle \delta v^j \delta \sigma^{ik} \rangle - \epsilon^{ij}, \quad (17)$$

$$\epsilon^{ij} = \langle \delta \sigma^{jk} \nabla_k \delta v^i \rangle + \langle \delta \sigma^{ik} \nabla_k \delta v^j \rangle. \quad (18)$$

The equation (14) also contains third-order moments of velocity fluctuations,

$$w^{ijk} = \langle \rho \delta v^i \delta v^j \delta v^k \rangle. \quad (19)$$

This quantity is usually associated with the diffusion of turbulence. Closures for the tensors (15)–(19) will be written later.

Finally, consider the gas energy balance. Denote by $\bar{\rho}K \equiv (1/2) w_k^k$ the volume density of the turbulence kinetic energy. From (14), (17) and (18) you can get

$$\begin{aligned} \frac{\partial (\bar{\rho}K)}{\partial t} + \nabla_k \left(\bar{\rho}K \bar{v}^k + \frac{1}{2} \varkappa_{ij} w^{ijk} - \langle \delta v_j \delta \sigma^{jk} \rangle \right) \\ = - w^{jk} \nabla_k \bar{v}_j + \frac{B_k^k}{2} - \frac{\Pi_k^k}{2} - \frac{\epsilon_k^k}{2}. \end{aligned} \quad (20)$$

Projecting (12) onto the mean velocity vector, we obtain the equation for the kinetic energy of the mean flow:

$$\begin{aligned} \frac{\partial}{\partial t} \left(\frac{\bar{\rho} |\bar{v}|^2}{2} \right) + \nabla_k \left(\frac{\bar{\rho} |\bar{v}|^2}{2} \bar{v}^k \right) \\ = - \bar{v}^k \nabla_k \bar{p} - \bar{v}_j \nabla_k w^{jk} + \bar{v}_j \nabla_k \langle \sigma^{jk} \rangle + \bar{v}_j \langle f^j \rangle. \end{aligned} \quad (21)$$

Averaging the equation for thermal energy (3), we obtain

$$\begin{aligned} \frac{\partial (\bar{\rho} \bar{e})}{\partial t} + \nabla_k [(\bar{\rho} \bar{e} + \bar{p}) \bar{v}^k + F_{\text{conv}}^k] \\ = \bar{v}^k \nabla_k \bar{p} + \langle \sigma^{jk} \rangle \nabla_k \bar{v}_j - \frac{B_k^k}{2} + \frac{\Pi_k^k}{2} + \frac{\epsilon_k^k}{2} + \langle q \rangle, \end{aligned} \quad (22)$$

and F_{conv}^k is the convective energy flux,

$$F_{\text{conv}}^k = \langle (\rho \delta e + \delta p) \delta v^k \rangle. \quad (23)$$

Adding (20), (21) and (22), we get the equation for the total energy:

$$\begin{aligned} \frac{\partial}{\partial t} \left(\frac{\bar{\rho} |\bar{v}|^2}{2} + \bar{\rho}K + \bar{\rho} \bar{e} \right) + \\ + \nabla_k \left[\left(\frac{\bar{\rho} |\bar{v}|^2}{2} + \bar{\rho}K + \bar{\rho} \bar{e} + \bar{p} \right) \bar{v}^k + (w^{jk} - \langle \sigma^{jk} \rangle) \bar{v}_j \right. \\ \left. + \frac{1}{2} \varkappa_{ij} w^{ijk} - \langle \delta v_j \delta \sigma^{jk} \rangle + F_{\text{conv}}^k \right] = \bar{v}_j \langle f^j \rangle + \langle q \rangle. \end{aligned} \quad (24)$$

As you can see, this equation is completely conservative, except for external sources. This means that the thermal and kinetic energy of the medium is redistributed between three flow components: mean, turbulent, and thermal. The momentum equations for momentum (2) and for thermal energy (3) include the microscopic viscous stress tensor σ^{ij} . It also enters the equation (14) through the dissipation tensor. Usually the microscopic viscosity does not affect large-scale accretion flows. However, it turns out to be critical in the process of establishing turbulence. Further, we will take into account microscopic viscosity only in the equation (14) for the turbulent stress tensor.

Continuity equation (8), equation of motion (12), energy (24) and turbulent stresses (14) constitute the main system of equations of the turbulent model we use.

2.2 Closure of the main system of equations

In the previous section, we wrote down the dynamic equation (14) for the w^{ij} tensor, which is the second moment tensor of velocity fluctuations. Similar equations can also be written for the tensors B^{ij} , Π^{ij} , X^{ij} , and w^{ijk} . However, they will contain moments of a higher order, and so on. The resulting problem of closing the chain of moments is usually solved by postulating some a priori connection between moments of different orders, using statistical considerations such as Wick's theorem, symmetry concepts, or empirical data. Dynamic equations for moments of the third and fourth orders can be seen, for example, in the works Canuto (1992, 1993, 1997) and others. In this paper, we use algebraic closures for the tensors Π^{ij} and X^{ij} . For convenience, we will further omit the line above the average values.

In order to write out a closed expression for the third-order velocity fluctuation moments w^{ijk} , (19), we use the gradient approximation:

$$\langle \rho \delta v^i \delta v^j \delta v^k \rangle = - \langle \delta v \ell \rangle (\nabla^i \langle \rho \delta v^j \delta v^k \rangle + \text{perm.}), \quad (25)$$

where ‘‘perm.’’ means cyclic permutations of indices i, j, k . The factor in this expression is interpreted as the coefficient of turbulent kinematic viscosity, which can be written as follows:

$$\nu_T \equiv \langle \delta v \ell \rangle = C_\nu t_T \frac{w_k^k}{2\rho}, \quad (26)$$

where t_T is the turbulence correlation time. The dimensionless factor C_ν in the gradient approximation is usually set equal to 0.09 (Launder 1974; Speziale 1991). As a result, the third moments are expressed in terms of the second moments and their derivatives:

$$w^{ijk} = - \nu_T (\nabla^i w^{jk} + \nabla^j w^{ki} + \nabla^k w^{ij}). \quad (27)$$

As can be seen from the equation (14), this tensor describes the diffusion of turbulence.

We noted above that under conditions of an accretion disk, Keplerian time seems to be a natural time scale for turbulence correlation. An estimate obtained by Stewart (1976) by analyzing an equation similar to (12) leads to an expression for the correlation time of the form

$$t_T = (1 + \mathcal{M}_T^{-2})^{1/2} \Omega_K^{-1}, \quad (28)$$

where Ω_K is the Keplerian angular velocity; \mathcal{M}_T is a turbulent Mach number, it depends on the local sound speed c_s^2 :

$$\mathcal{M}_T^2 = \frac{w_k^k}{\rho c_s^2}. \quad (29)$$

Finally we have

$$\nu_T = \mathbb{C}_\nu \mathcal{M}_T (1 + \mathcal{M}_T^2)^{1/2} \frac{c_s^2}{2\Omega_K}. \quad (30)$$

Mach numbers estimated from the nonthermal broadening of spectral lines in protoplanetary disks can be from 0.06 and even lower (Flaherty et al. 2017) to 0.5 (Guilloteau et al. 2012), which gives estimates for turbulence correlation time within $0.3 \lesssim t_T \Omega_K / (2\pi) \lesssim 2.7$.

The quantity $\rho \langle \delta v^i \rangle$ in the B^{ij} tensor, (15), is the convective mass flux. Using the definitions (6) and (7) it can be rewritten as $-\langle \delta \rho \delta v^i \rangle$. Convection is a rather slow process, so we can use the Boussinesq approximation and express density fluctuations in terms of temperature fluctuations at constant pressure (Landau & Lifshitz 1959):

$$\delta \rho = \left(\frac{\partial \rho}{\partial T} \right)_p \delta T = -\alpha_{\text{vol}} \rho \delta T, \quad (31)$$

where α_{vol} is the coefficient of volume expansion, for gases it is approximately equal to $1/T$. In thermal convection models, the convective flux (23) is usually written as

$$F_{\text{conv}}^i = C_p \langle \rho \delta T \delta v^i \rangle. \quad (32)$$

Taking (31) into account, we get $\rho \langle \delta v^i \rangle = (C_p T)^{-1} F_{\text{conv}}^i$. The buoyancy tensor in this approximation takes the form

$$B^{ij} = -\frac{1}{C_p T} \left(\frac{\nabla^i p}{\rho} F_{\text{conv}}^j + \frac{\nabla^j p}{\rho} F_{\text{conv}}^i \right). \quad (33)$$

Note that the r.h.s of the equations (20) and (22) contains the convective source B_k^k . Under the conditions of an accretion disk, one can expect that the pressure gradient is directed towards the disk midplane, while the convective flow is directed away from it. Hence, we can conclude that $B_k^k \geq 0$, which means that convection transforms the thermal energy of the mean flow into turbulence.

It is generally accepted that pressure fluctuations play a key role in the development of turbulence. In the tensor Π^{ij} , (16), these effects manifest themselves through the isotropization of turbulence (“return-to-isotropy”), buoyancy and interaction with the background flow. Considerations of symmetry and dimension (see references in Launder (1974), Speziale (1991) and Canuto (1997)) led to the following form of this tensor (recall that \varkappa^{ij} are the components of the metric):

$$\begin{aligned} \Pi^{ij} = & \frac{\mathbb{C}_{\Pi 1}}{t_T} b^{ij} - \mathbb{C}_{\Pi 2} \left(b^{ik} U_k^j + b^{jk} U_k^i - \frac{2}{3} b^{kl} U_{kl} \varkappa^{ij} \right) \\ & - \mathbb{C}_{\Pi 3} \varkappa_{kl} (b^{ik} V^{jl} + b^{jk} V^{il}) - \left(U^{ij} - \frac{U_l^l}{3} \varkappa^{ij} \right) \frac{2w_k^k}{5} \\ & + (1 - \mathbb{C}_B) B^{ij}, \end{aligned} \quad (34)$$

where b^{ij} characterizes the deviation from isotropy,

$$b^{ij} = w^{ij} - \frac{w_k^k}{3} \varkappa^{ij}. \quad (35)$$

U^{ij} and V^{ij} are, respectively, the symmetric and asymmetric parts of the strain rate tensor of the background flow,

$$U^{ij} = \frac{1}{2} \left(\nabla^j v^i + \nabla^i v^j \right), \quad (36)$$

$$V^{ij} = \frac{1}{2} \left(\nabla^j v^i - \nabla^i v^j \right). \quad (37)$$

Note that, except for the last term, the expression (34) depends linearly on the components of the Reynolds tensor.

Turbulence dissipation occurs on small scales, where the anisotropy is weak in average. For this reason, the conservative part of the X^{ij} tensor in the (17) equation is usually neglected, then only the purely dissipative part remains, i.e. $X^{ij} = -\epsilon^{ij}$. From the same considerations of isotropy on the dissipation scale, this tensor is usually written in the form

$$\epsilon^{ij} = \frac{2}{3} \epsilon \varkappa^{ij}, \quad (38)$$

where it follows from the definition (18) that $\epsilon = \langle \delta \sigma^{jk} \nabla_k \delta v_j \rangle$. For the scalar quantity ϵ we take the classical closure of the form

$$\epsilon = \frac{K}{t_T}, \quad (39)$$

and $K = (1/2) w_k^k$.

The constants in the expressions (26) and (34) were obtained experimentally, see papers Launder (1974), Speziale (1991), Canuto (1992, 1993), and references therein:

$$\mathbb{C}_\nu = 0.09, \quad \mathbb{C}_B = 0.6, \quad (40)$$

$$\mathbb{C}_{\Pi 1} = 3.5, \quad \mathbb{C}_{\Pi 2} = 0.61, \quad \mathbb{C}_{\Pi 3} = 0.44. \quad (41)$$

2.3 Convective flux and conditions for instability

In the mixing length theory, the heat transfer is carried out by convective elements, which are formed as a result of convective instability. For simplicity, we imagine that the elements move under the action of the buoyancy force with a certain characteristic speed v_{conv} and transfer the excess heat $\rho C_p \Delta T$ to the environment. The convective energy flux can be written as $\rho C_p \Delta T v_{\text{conv}}$. Different versions of the theory differ in the ways of estimating the quantities ΔT and v_{conv} . In this case, radiative heat losses by the convective element, its viscous deceleration and “transfer” of convection beyond the convective zone (overshooting) (Canuto 1992) can be taken into account.

The conditions for convective instability are satisfied in those regions where the temperature gradient exceeds the adiabatic (more precisely, isentropic) gradient in the direction opposite to the gravitational acceleration. Let us denote the excess gradient of the temperature

$$\beta^i = - \left[n^i n_k \nabla^k T - (\nabla^i T)_{\text{ad}} \right], \quad (42)$$

where n^i is the unit vector in the direction of the gravitational acceleration vector g^i . The adiabatic gradient is also expressed in terms of the acceleration vector,

$$(\nabla^i T)_{\text{ad}} = \frac{g^i}{C_p}. \quad (43)$$

The condition for the onset of instability has the form $-g_k \beta^k > 0$. It should be noted that the centrifugal acceleration also contributes to the value of g^i .

Let us write down the results given in [Hansen & Kawaler \(1994\)](#) for the problem of stellar convection without detailed derivation. The characteristic parameter of the theory is the length of the mixing path ℓ — the path that the convective element travels before it mixes with the surrounding matter. In models of convective stars, this quantity is usually associated with the pressure scale. The intensity of convection is also characterized by the increment of convective instability

$$\omega = -\frac{\nu_{\text{mol}} + \nu_{\text{rad}}}{2\ell^2} + \left[\frac{(\nu_{\text{mol}} + \nu_{\text{rad}})^2}{4\ell^4} + |\mathcal{N}|^2 \right]^{1/2}, \quad (44)$$

where ν_{mol} and ν_{rad} are the molecular (collisional) and radiative thermometric conductivity, respectively, cm^2/s ; \mathcal{N} is the Brunt-Väisälä frequency, it is defined as

$$\mathcal{N}^2 = \frac{g_k \beta^k}{T}. \quad (45)$$

In a convectively stable medium ($g_k \beta^k > 0$), \mathcal{N} is the oscillation frequency of the gas element due to buoyancy. Note that in the limit of weak convection, $|\mathcal{N}|^2 \rightarrow 0$, we have $\omega \approx |\mathcal{N}|^2 \ell^2 / (\nu_{\text{mol}} + \nu_{\text{rad}})$, in the limit of strong convection, $|\mathcal{N}|^2 \rightarrow \infty$, we get $\omega \approx |\mathcal{N}|$. The speed of the convective elements and the excess temperature are estimated as follows:

$$v_{\text{conv}}^i = \omega \ell n^i, \quad (46)$$

$$\Delta T = \frac{\omega^2}{|\mathcal{N}|^2} \ell \beta. \quad (47)$$

As a result, the convective energy flux takes the form

$$F_{\text{conv}}^i = \rho C_p \frac{\omega^3}{|\mathcal{N}|^2} \ell^2 \beta^i. \quad (48)$$

We write the coefficient of collisional thermometric conductivity in the form

$$\nu_{\text{mol}} = \frac{1}{\rho C_p} \frac{\mu m_{\text{H}} C_v v_{\text{th}}}{3\sigma_{\text{nn}}}, \quad (49)$$

where $v_{\text{th}} = [3k_{\text{B}}T/(\mu m_{\text{H}})]^{1/2}$ is the average thermal velocity of molecules; $\sigma_{\text{nn}} = 3 \times 10^{-16} \text{ cm}^2$ is the collision cross section for neutral hydrogen. The coefficient of radiative thermometric conductivity has the form

$$\nu_{\text{rad}} = \frac{1}{\rho C_p} \frac{4ca_{\text{rad}}T^3}{3\rho\kappa_{\text{R}}}, \quad (50)$$

where $a_{\text{rad}} = 7.56 \times 10^{-15} \text{ erg cm}^{-3} \text{ K}^{-4}$ is the radiation density constant; κ_{R} is the Rosseland-averaged opacity. We note that in many astrophysical applications the collisional mechanism of heat conduction can be neglected.

The model of a convective flow of the form (48) has one free parameter — the length of the mixing path ℓ . The dependence on this parameter is quite strong: from ℓ^4 in the limit of weak convection to ℓ^2 for strong convection. In models of convective shells of stars, the pressure scale of the star is usually taken as the length of the mixing length. Under the conditions of an accretion disk, the vertical thermal scale of the disk can be taken as the mixing length.

3 ONE-DIMENSIONAL MODEL OF TURBULENT CONVECTION IN A PROTOPLANETARY DISK

3.1 One-dimensional model and derivation of a final system of equations

Let us write together the basic dynamic equations of turbulent flow:

$$\frac{\partial \rho}{\partial t} + \nabla_k(\rho v^k) = 0, \quad (51)$$

$$\frac{\partial(\rho v^i)}{\partial t} + \nabla_k(\rho v^i v^k) = -\nabla^i p - \nabla_k w^{ik} + \rho g^i, \quad (52)$$

$$\begin{aligned} \frac{\partial(\rho e)}{\partial t} + \nabla_k(\rho e v^k) \\ = -p \nabla_k v^k - \nabla_k F_{\text{conv}}^k - C_B \frac{B_k^k}{2} + \epsilon + q, \end{aligned} \quad (53)$$

$$\begin{aligned} \frac{\partial w^{ij}}{\partial t} + \nabla_k(w^{ij} v^k) + \nabla_k w^{ijk} \\ = -(w^{ik} \nabla_k v^j + w^{jk} \nabla_k v^i) + B^{ij} - \Pi^{ij} - \frac{2}{3} \epsilon \mathcal{K}^{ij}. \end{aligned} \quad (54)$$

Compared to the equations (12), (22), (14) that we wrote earlier, here changes were made: in the laws of conservation of momentum and thermal energy, we neglected the microscopic viscosity as well as the conservative part of the turbulent dissipation tensor (see section 2.2), and also explicitly wrote out the trace Π_k^k . To the system of equations (51)–(54), it is necessary to add the closures from the 2.2 section, the expression for the convective flow (48), as well as define the gravitational acceleration g^i and define the source of thermal energy q , which will be determined by radiative processes.

Set a cylindrical coordinate system¹ (r, ϕ, z) and consider a rotational axisymmetric flow in a narrow radial annulus of radius r . We require that all quantities do not depend on the azimuth angle. We will assume that the disk is in a state close to mechanical equilibrium. The magnitudes of the gradients can be estimated as

$$\frac{\partial}{\partial r} \lesssim \frac{\partial}{\partial z} \sim \frac{1}{H} \sim \frac{|\Omega|}{c_s}, \quad (55)$$

where H is the vertical thermal scale in the disk; $\Omega \equiv v_\phi/r$ is the angular velocity of gas rotation. If flare states are not considered, then in typical accretion disks, the radial and vertical velocities of gas motion are substantially subsonic. In this case

$$|v_r| \sim |v_z| \equiv \mathcal{M} c_s, \quad (56)$$

$$\left| \frac{\partial v_r}{\partial r} \right| \sim \left| \frac{\partial v_r}{\partial z} \right| \sim \left| \frac{\partial v_z}{\partial r} \right| \sim \left| \frac{\partial v_z}{\partial z} \right| \sim \frac{\mathcal{M} c_s}{H} \sim \mathcal{M} |\Omega|. \quad (57)$$

where $\mathcal{M} \ll 1$ is the Mach number for the radial and vertical gas velocities. In this approximation, advection terms in the expressions (52)–(54) can be neglected, except for the centrifugal force in the Euler equation, as well as the components corresponding to it in the turbulence transport equation. Let us neglect the radial dependence for all quantities, except for the angular velocity of the flow. We will take into account only the gravity of the star, neglecting the self-gravity of the disk. Finally, the system of equations

¹ Further, all vector and tensor quantities will be written in locally Cartesian projections.

(52)–(54) will take the following form:

$$\frac{\partial p}{\partial z} = \rho \Omega_K^2 z - \frac{\partial w_{zz}}{\partial z}, \quad (58)$$

$$\rho C_v \frac{\partial T}{\partial t} = -\frac{\partial F_{\text{conv}}}{\partial z} - \frac{C_B}{2} B_{zz} + \epsilon + q, \quad (59)$$

$$\frac{\partial w_{rr}}{\partial t} = \frac{\partial}{\partial z} \left(\nu_T \frac{\partial w_{rr}}{\partial z} \right) - \Pi_{rr} + 4\Omega w_{r\phi} - \frac{2\epsilon}{3}, \quad (60)$$

$$\frac{\partial w_{\phi\phi}}{\partial t} = \frac{\partial}{\partial z} \left(\nu_T \frac{\partial w_{\phi\phi}}{\partial z} \right) - \Pi_{\phi\phi} - \frac{2}{r} \frac{\partial(r^2 \Omega)}{\partial r} w_{r\phi} - \frac{2\epsilon}{3}, \quad (61)$$

$$\frac{\partial w_{zz}}{\partial t} = \frac{\partial}{\partial z} \left(3\nu_T \frac{\partial w_{zz}}{\partial z} \right) - \Pi_{zz} + B_{zz} - \frac{2\epsilon}{3}, \quad (62)$$

$$\frac{\partial w_{r\phi}}{\partial t} = \frac{\partial}{\partial z} \left(\nu_T \frac{\partial w_{r\phi}}{\partial z} \right) - \Pi_{r\phi} - \frac{1}{r} \frac{\partial(r^2 \Omega)}{\partial r} w_{rr} + 2\Omega w_{\phi\phi}, \quad (63)$$

$$\frac{\partial w_{rz}}{\partial t} = \frac{\partial}{\partial z} \left(2\nu_T \frac{\partial w_{rz}}{\partial z} \right) - \Pi_{rz} + 2\Omega w_{\phi z}, \quad (64)$$

$$\frac{\partial w_{\phi z}}{\partial t} = \frac{\partial}{\partial z} \left(2\nu_T \frac{\partial w_{\phi z}}{\partial z} \right) - \Pi_{\phi z} - \frac{1}{r} \frac{\partial(r^2 \Omega)}{\partial r} w_{rz} - \Omega w_{\phi z}. \quad (65)$$

In these equations, Ω_K is the Keplerian angular velocity at radius r ; ν_T is the turbulent viscosity coefficient (30).

By virtue of the chosen approximation, only the z -component of the convective flux vector (48) remains nonzero and, as a consequence, the only nonzero component of the buoyancy tensor:

$$B_{zz} = -\frac{2}{C_p \rho T} \frac{\partial p}{\partial z} F_{\text{conv}}. \quad (66)$$

The components of the isotropization tensor are

$$\Pi_{rr} = \frac{C_{\Pi 1}}{t_T} b_{rr} - \left(\frac{2C_{\Pi 2}}{3} U_{r\phi} - 2C_{\Pi 3} V_{r\phi} \right) b_{r\phi}, \quad (67)$$

$$\Pi_{\phi\phi} = \frac{C_{\Pi 1}}{t_T} b_{\phi\phi} - \left(\frac{2C_{\Pi 2}}{3} U_{r\phi} + 2C_{\Pi 3} V_{r\phi} \right) b_{r\phi}, \quad (68)$$

$$\Pi_{zz} = \frac{C_{\Pi 1}}{t_T} b_{zz} + \frac{4C_{\Pi 2}}{3} U_{r\phi} b_{r\phi} + (1 - C_B) B_{zz}, \quad (69)$$

$$\Pi_{r\phi} = \frac{C_{\Pi 1}}{t_T} b_{r\phi} - C_{\Pi 2} U_{r\phi} (b_{rr} + b_{\phi\phi}) - C_{\Pi 3} V_{r\phi} (b_{rr} - b_{\phi\phi}) - \frac{4}{5} U_{r\phi} K, \quad (70)$$

$$\Pi_{rz} = \frac{C_{\Pi 1}}{t_T} b_{rz} - (C_{\Pi 2} U_{r\phi} - C_{\Pi 3} V_{r\phi}) b_{\phi z}, \quad (71)$$

$$\Pi_{\phi z} = \frac{C_{\Pi 1}}{t_T} b_{\phi z} - (C_{\Pi 2} U_{r\phi} + C_{\Pi 3} V_{r\phi}) b_{rz}, \quad (72)$$

where

$$b_{rr} = \frac{1}{3} (2w_{rr} - w_{\phi\phi} - w_{zz}), \quad (73)$$

$$b_{\phi\phi} = \frac{1}{3} (2w_{\phi\phi} - w_{rr} - w_{zz}), \quad (74)$$

$$b_{zz} = \frac{1}{3} (2w_{zz} - w_{rr} - w_{\phi\phi}), \quad (75)$$

$$b_{r\phi} = w_{r\phi}, \quad b_{rz} = w_{rz}, \quad b_{\phi z} = w_{\phi z}, \quad (76)$$

$$K = \frac{1}{2} (w_{rr} + w_{\phi\phi} + w_{zz}), \quad (77)$$

$$U_{r\phi} = \frac{r}{2} \frac{\partial \Omega}{\partial r}, \quad V_{r\phi} = -\frac{1}{2r} \frac{\partial(r^2 \Omega)}{\partial r}. \quad (78)$$

As can be seen from the expressions (60)–(65), the only

source of turbulence is the convective heat flux in the equation (62). The background flow participates only in strengthening or weakening of various w_{ij} components.

There are several sources on the right side of the heat balance equation (59): the first one is responsible for the convective heat transfer, the second one describes the consumption of thermal energy for convective motions, the third one provides energy inflow due to turbulence dissipation. The last source, q , takes into account heating by stellar and interstellar radiation, the exchange of thermal energy with its own IR radiation, and can also include an additional heat source. The model for calculating q will be described in the next section.

The (60)–(65) equations must be provided with boundary conditions. On the upper boundary of the disk, it is natural to set all w_{ij} to zero. In the disk midplane ($z = 0$), the boundary conditions are:

$$\frac{\partial w_{rr}}{\partial z} = \frac{\partial w_{\phi\phi}}{\partial z} = \frac{\partial w_{zz}}{\partial z} = \frac{\partial w_{r\phi}}{\partial z} = 0, \quad (79)$$

$$w_{rz} = w_{\phi z} = 0. \quad (80)$$

It can be seen that in the system (60)–(65) the last two equations do not contain an energy source or sink and describe only the redistribution of turbulent energy between components w_{rz} and $w_{\phi z}$. Taking into account the boundary conditions, this means that if these components were initially zero, they will be zero in the future as well. On this basis, the equations for the quantities w_{rz} and $w_{\phi z}$ will not be considered further. Under the conditions of an accretion disk, we take the mixing length equal to the vertical thermal scale of the disk, $\ell \equiv H = c_s/|\Omega|$.

The solution of the complete system of equations (58)–(65) was performed on a spatial grid with a dimension of 1000 cells. For each time step, the state of the disk was calculated in two stages. At the first stage, the gas temperature field, the radiation field, and the convective flow were calculated by jointly solving the equation of heat transfer, radiative transfer, and hydrostatics. At the second stage, the turbulent transport and the corresponding heat source were calculated. The heat and radiative transport were calculated by a completely implicit scheme using iterations, and the transport of turbulence was computed by an explicit-implicit scheme.²

3.2 Combining the turbulent convection model with the radiative transfer model

The calculation of radiative transfer and self-consistent calculation of the source q included in the heat balance equation (59) is carried out using the thermal model from VoroByov & Pavlyuchenkov (2017) and Pavlyuchenkov et al. (2020). In the framework of their model, when calculating q , the exchange of thermal energy with intrinsic IR radiation, heating

² The model was implemented on PYTHON 3.7 (Van Rossum & Drake 2009) + NUMPY (Harris et al. 2020) + SCIPY (Virtanen et al. 2020) + NUMBA (Lam et al. 2015) + NUMBALSODA (Wogan & Rackauckas 2022). The solution of the turbulence transfer equation was carried out according to an explicit-implicit scheme using the LSODA algorithm (Petzold 1983).

by stellar and interstellar radiation S_{UV} , and an additional source of heat release S_{ext} are taken into account:

$$q = c\rho\kappa_{\text{P}}(E_{\text{rad}} - a_{\text{rad}}T^4) + \rho S_{\text{UV}} + \rho S_{\text{ext}}, \quad (81)$$

where E_{rad} is the energy density of IR radiation; a_{rad} is the Stefan-Boltzmann constant; κ_{P} is the Planck-averaged absorption coefficient. The S_{ext} source can be associated with some dissipative processes that are not explicitly involved in our model; this background source is the main convection driving factor. Heating by stellar and interstellar radiation, S_{UV} , is calculated by direct integration of radiation transfer. To simulate the IR transfer, the Eddington approximation is used, which reduces to the following system of equations:

$$\frac{\partial E_{\text{rad}}}{\partial t} + \frac{\partial F_{\text{rad}}}{\partial z} = -c\rho\kappa_{\text{P}}(E_{\text{rad}} - a_{\text{rad}}T^4), \quad (82)$$

$$F_{\text{rad}} = -\frac{c}{3\rho\kappa_{\text{R}}}\frac{\partial E_{\text{rad}}}{\partial z}, \quad (83)$$

where F_{rad} is the IR radiation flux; κ_{R} is the Rosseland-averaged absorption coefficient. The boundary conditions for the radiation flux at the midplane and at the upper boundary z_{max} have the form:

$$\left.\frac{\partial F_{\text{rad}}}{\partial z}\right|_{z=0} = 0, \quad (84)$$

$$\left.\frac{\partial F_{\text{rad}}}{\partial z}\right|_{z=z_{\text{max}}} = \frac{c}{2}\left(E_{\text{rad}}\Big|_{z=z_{\text{max}}} - a_{\text{rad}}T_{\text{CMB}}^4\right), \quad (85)$$

where $T_{\text{CMB}} = 2.73$ K. An important feature of the used thermal disk model is that it uses temperature-dependent Rosseland and Planck-averaged opacities. These opacities were obtained for the absorption and scattering coefficients of a mixture of graphite-silicon dust grains and were also borrowed from Pavlyuchenkov et al. (2020), where it was noted that an increase in opacity with temperature is a necessary condition for the onset of convection. The solution of the subsystem of radiative transfer equations (81)–(83) is found using an implicit method, the details of which are described in the appendix of the article Vorobyov & Pavlyuchenkov (2017).

We noted above that convection in our model is the only source of turbulence. In this case, to start convection in the disk, an external heat source is required, which is included in the heat balance equation (59), (81). We introduce it formally through the accretion rate \dot{M} , which is independent of time (Shakura & Sunyaev 1973):

$$S_{\text{ext}} = \left|\frac{d\ln\Omega}{d\ln r}\right| \frac{\dot{M}\Omega^2}{4\pi\Sigma}, \quad (86)$$

where Σ is the local surface density of the disk.

Figure 2 shows an example of calculating the thermal structure of a protoplanetary disk within the framework of the radiation transfer model used (without modeling convection and turbulence). The main parameters of this model: the mass of the star $1 M_{\odot}$, the effective temperature of the star 5780 K, the rate of accretion onto the star $10^{-4} M_{\odot} \text{ yr}^{-1}$, the power distribution law of the surface density $\Sigma \propto r^{-1}$ and density 10^3 g cm^{-2} at a radius of 1 au. In this calculation, the convective flow did not participate in the formation of the thermal structure of the disk, but was calculated from the resulting density and temperature distributions. The bottom two graphs show the region of con-

Table 1. Parameters of Disk Models with Turbulent Convection

Star mass	M_{s}	$1 M_{\odot}$
Star radius	R_{s}	$1 R_{\odot}$
Star effective temperature	T_{s}	5780 K
Radial distance of the column	r	3.34 au
Gas molecular weight	μ	2.3
Gas adiabatic exponent	γ	7/5
Disk surface density	Σ	542.29 g cm^{-2}
Gas number density		
at the external boundary	n_{ext}	10^3 cm^{-3}
ISM radiation temperature	T_{ISR}	10^4 K
Accretion rate (model ‘A’)	\dot{M}	$10^{-7} M_{\odot} \text{ yr}^{-1}$
(model ‘B’)	\dot{M}	$10^{-4} M_{\odot} \text{ yr}^{-1}$

vective instability ($\nabla - \nabla_{\text{ad}} > 0$)³, convective flow in which is not equal to zero. The maximum value of the convective flow is reached at the radius $r = 3.34$ au, and the maximum density and temperature are reached approximately at the same radius. We will choose this radius as the radius of the ring for the one-dimensional model with the calculation of turbulent convection.

3.3 Considered disk models with turbulent convection

Within the framework of the one-dimensional turbulent disk convection, the vertical structure was modeled for a column located at a distance of $r = 3.34$ au from the star. The main parameters of the model are listed in the Table 1. We considered options with accretion rate $\dot{M} = 10^{-7} M_{\odot} \text{ yr}^{-1}$ (model ‘A’) and $\dot{M} = 10^{-4} M_{\odot} \text{ yr}^{-1}$ (pattern ‘B’). These options correspond to a quiescent and flash state of the disk, respectively. For both states, two runs were performed: with no convection hence, no turbulence, and the full model, with convection and turbulence. All calculations were carried out from the initial isothermal distribution of gas with a temperature of 100 K and without turbulence, until a steady state was reached.

The results of the calculation of model ‘A’ are shown in Fig. 3. As can be seen, a convective flow arises in the disk, while the boundary of the convective zone extends upward to approximately one and a half scales of thermal height. In a significant part of the convective zone, the convective flow turns out to be comparable in magnitude to the radiative flow. Thus, convection provides about half of the total heat flow. The total energy flux is only a few percent higher than the energy flux in the calculation without convection (dashed lines). This, however, is enough to reduce the temperature of the inner layers of the disk, within the thermal scale, by about 25 K.

In our model, the convective flow is directed along the Oz axis, so the convection directly excites only the w_{zz} component of the Reynolds tensor. The remaining components of this tensor arise from w_{zz} both due to the pressure tensor Π_{ij} and through interaction with the background flow. Note that w_{zz} dominates in magnitude, it exceeds w_{rr} and

³ This is how the excess temperature gradient with respect to pressure is denoted: $\nabla - \nabla_{\text{ad}} = dT/dp - (dT/dp)_{\text{ad}}$. This gradient is calculated along the action of the buoyancy force (in our case, along the Oz axis).

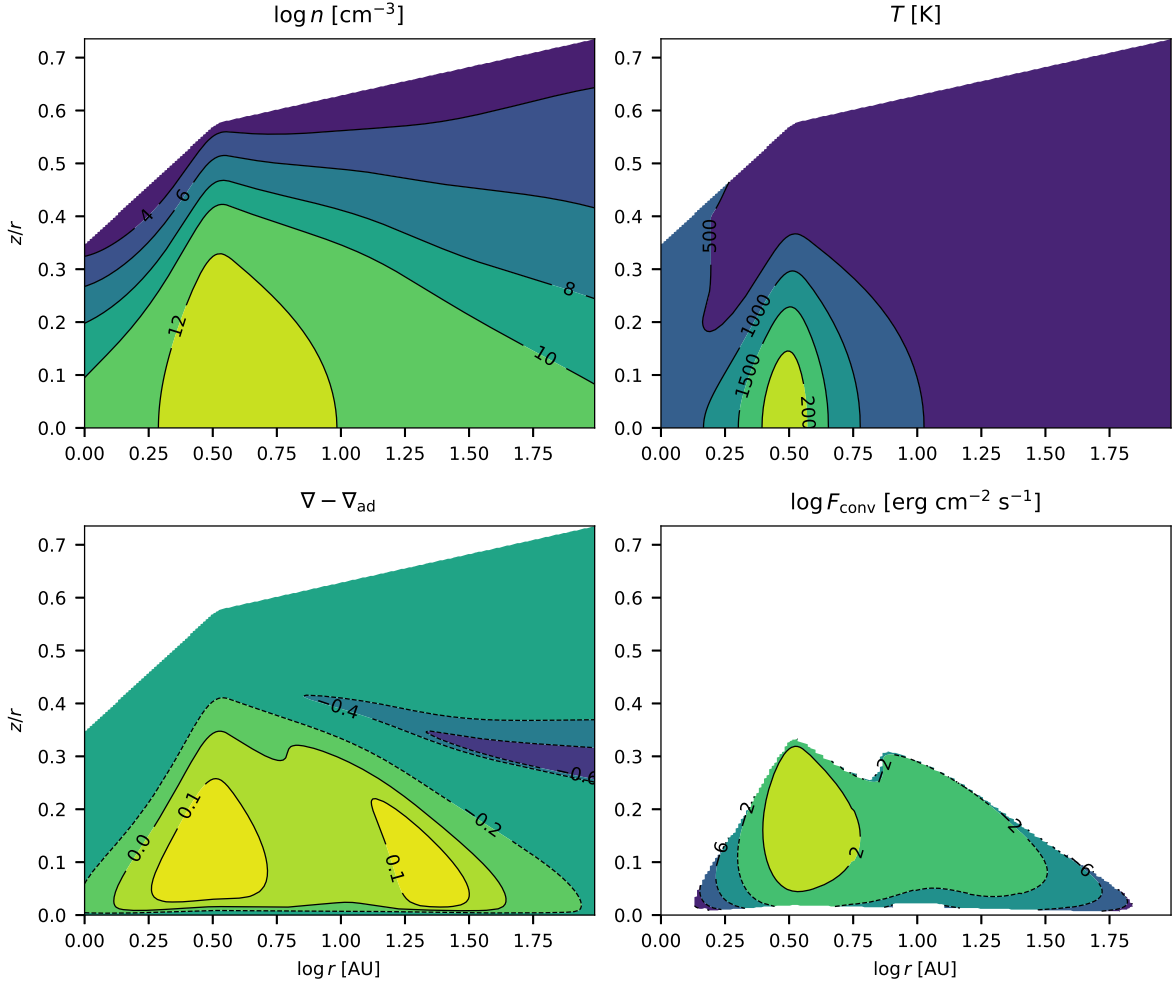


Figure 2. The structure of a protoplanetary disk without calculating turbulent convection: gas number density (*upper left panel*), temperature (*upper right panel*), excess temperature gradient over pressure (*lower left panel*) and the magnitude of the convective flow (*bottom right panel*).

$w_{\phi\phi}$ by 3–5 times and exceeds $w_{r\phi}$ by two or more orders of magnitude. The intensity of turbulence and the corresponding contribution to the width of the observed spectral lines is determined by the trace of the Reynolds tensor, $\sum_k w_{kk}$. Due to turbulent diffusion, the region of developed turbulence is almost twice as thick as the convective zone. In the bulk of the disk material, the Mach number \mathcal{M}_T varies in the range 0.03–0.08, which is in good agreement with the estimates obtained from observations (Flaherty et al. 2017).

The rate of removal of angular momentum due to turbulence and the corresponding rate of accretion (which we will call effective) depend on the off-diagonal component $w_{r\phi}$ (Shakura & Sunyaev 1973):

$$\dot{M}_{\text{eff}} = \frac{2\pi}{|\Omega|} W_{r\phi}, \quad (87)$$

$$W_{r\phi} = 2 \int_0^{z_{\text{max}}} w_{r\phi} dz. \quad (88)$$

The effective accretion rate can be estimated in terms of the

alpha parameter:

$$\alpha_{\text{eff}} = \frac{W_{r\phi}}{P}, \quad (89)$$

$$P = 2 \int_0^{z_{\text{max}}} \frac{\mathcal{R}}{\mu} \rho T dz. \quad (90)$$

As you can see, due to the fact that $w_{r\phi} \ll \sum_k w_{kk}$ (see Fig. 3 and table 2), one cannot draw a right conclusion about the accretion rate from the turbulent kinetic energy. In model ‘A’, the effective accretion rate is $\dot{M}_{\text{eff}} = 1.71 \times 10^{-10} M_{\odot} \text{ yr}^{-1}$, which is 1000 times less than the accretion rate \dot{M} , through which the heating of the layer was set.

On Fig. 3 (middle row, right column) shows the distribution of external heating sources $\rho(S_{\text{ext}} + S_{\text{UV}})$, as well as the source associated with convection ρS_{conv} and with turbulent dissipation, ρS_{turb} :

$$\rho S_{\text{conv}} = -\frac{\partial F_{\text{conv}}}{\partial z} - \frac{C_B}{2} B_{zz}, \quad (91)$$

$$\rho S_{\text{turb}} = \epsilon. \quad (92)$$

In the inner layers of the disk, $z < 0.5$ au, the external

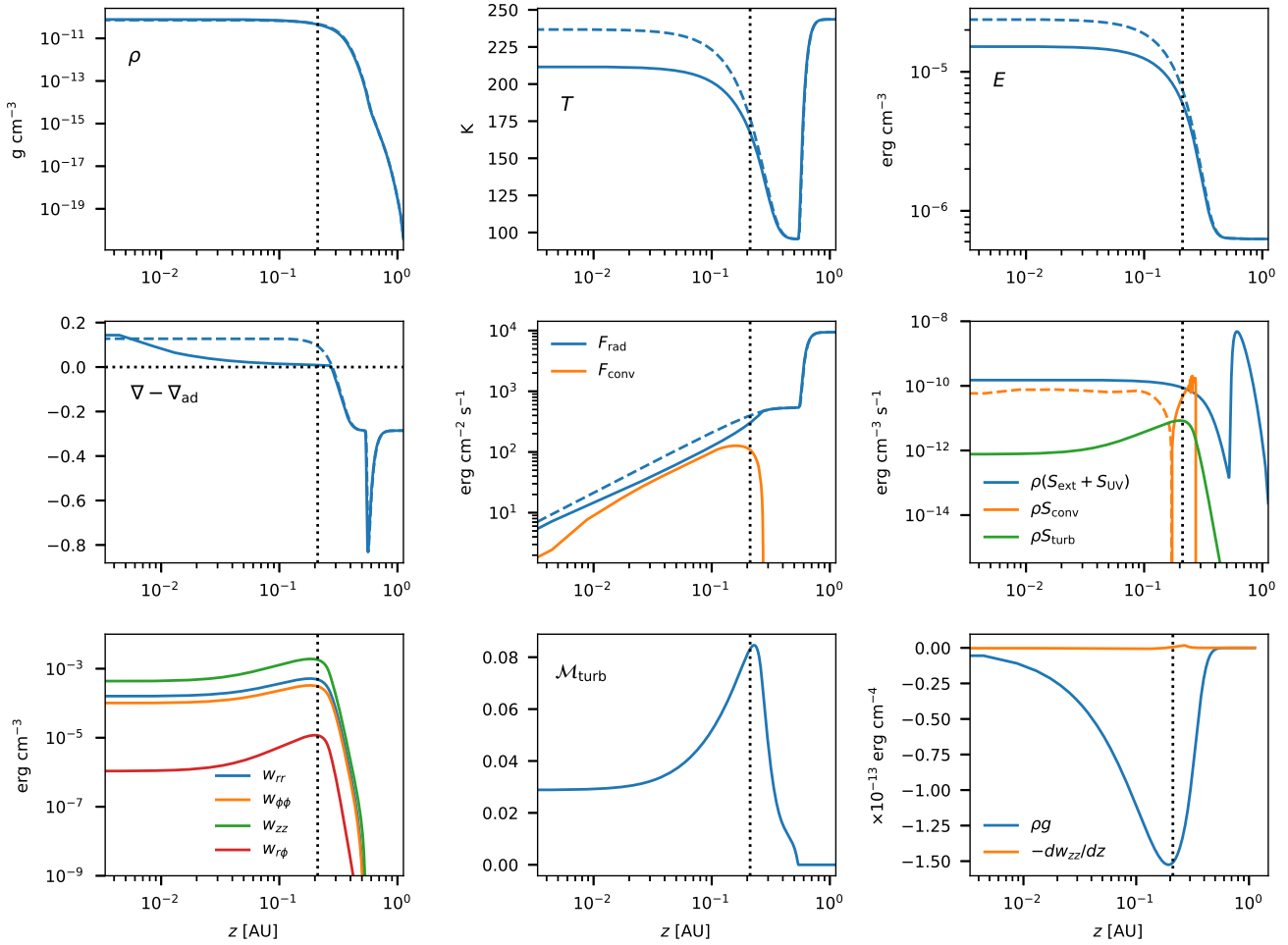


Figure 3. The model ‘A’ results, $\dot{M} = 10^{-7} M_{\odot} \text{yr}^{-1}$. Top row, from left to right: density, temperature, bulk radiation density. Middle row: excess of temperature gradient over pressure, energy flux, volumetric heat source (yellow dashed line denotes negative ρS_{conv} values). Bottom row: turbulent stress tensor components, turbulent Mach number and volumetric force density. The blue dashed lines indicate the results of the model without taking into account convection. Dotted vertical lines mark the thermal scale of the disk.

source ρS_{ext} dominates among all sources, except for a narrow region near the boundary of the thermal scale, where the convective source ρS_{conv} is more important. Heating from a convective source is comparable to external heating in absolute value, but its role is to redistribute and slightly reduce thermal energy. The source ρS_{turb} associated with turbulence dissipation is everywhere smaller than ρS_{ext} by one or two orders of magnitude. The integral values of each of the sources ($Q = 2 \int_0^{z_{\text{max}}} \rho S dz$) are given in Table 2. Also note that in model ‘A’ even more energy is spent to start convection than is returned to the heat budget from dissipation: $|Q_{\text{conv}}| > Q_{\text{turb}}$.

In the case of higher heating power Q_{ext} , which corresponds to the accretion rate $\dot{M} = 10^{-4} M_{\odot} \text{yr}^{-1}$, convection also develops. The value of the convective flow in model ‘B’ is much higher than in model ‘A’, but is much lower than the radiative flow and does not affect the thermal structure of the layer. The amplitude of turbulent fluctuations at the maximum, which is located near the upper boundary of the vertical thermal scale, exceeds $0.2 c_s$, see Fig. 4. However, the $w_{r\phi}$ tensor component responsible for the transfer of an-

Table 2. Results obtained for models ‘A’ and ‘B’.

		Model ‘A’	Model ‘B’
\dot{M}	$M_{\odot} \text{yr}^{-1}$	10^{-7}	10^{-4}
\dot{M}_{eff}	”	1.71×10^{-10}	1.68×10^{-8}
Q_{UV}	$\text{erg cm}^{-2} \text{s}^{-1}$	1.77×10^4	1.77×10^4
Q_{ext}	”	1.07×10^3	1.07×10^6
Q_{conv}	”	-4.30×10^1	-3.92×10^3
Q_{turb}	”	3.98×10^1	4.17×10^3
$\dot{M}_{\text{eff}}/\dot{M}$		1.71×10^{-3}	1.68×10^{-4}
$Q_{\text{turb}}/Q_{\text{ext}}$		3.72×10^{-2}	3.90×10^{-3}
$W_{r\phi}/(\sum_i W_{ii})$		3.52×10^{-3}	7.93×10^{-3}
α_{eff}		1.55×10^{-5}	1.51×10^{-4}

gular momentum is two orders of magnitude smaller than the w_{zz} component, as in the ‘A’ model. The contrast between the value of the given accretion rate, which actually determines the source of external heating (86) and the effective one is an order of magnitude smaller than in the ‘A’ model and is 1.68×10^{-4} , see Table 2.

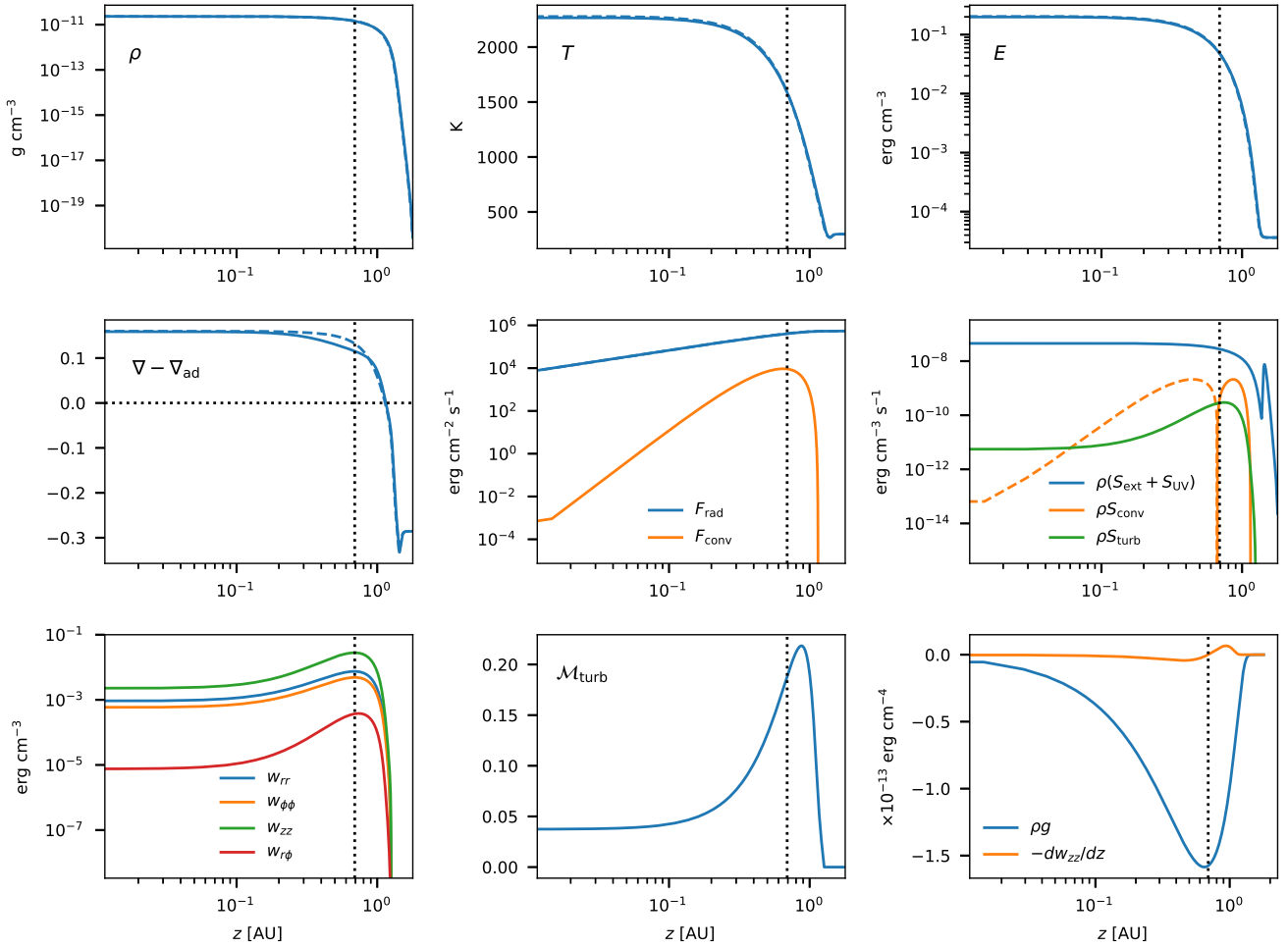


Figure 4. The model ‘B’ results, $\dot{M} = 10^{-4} M_{\odot} \text{ yr}^{-1}$. Line designations are the same as in Fig. 3

4 DISCUSSION AND CONCLUSION

The paper presents a model for the transport of anisotropic turbulence in an accretion disk in the mean field approximation. This model was developed to study turbulence of various nature and its role in the redistribution of the angular momentum of the accretion disk. The mean field approach makes it possible to take into account various types of instabilities by adding appropriate sources in the form of fluctuation correlators of hydrodynamic quantities. In addition to the transfer of angular momentum, turbulence in protoplanetary disks can also lead to other consequences, for example, mixing of chemical components in gas and dust, which can change the heat balance in the disk. These effects are also easy to take into account in the model. The model was used by us to study the role of convective instability within the one-dimensional approximation. To do this, it was combined with the calculation of radiative transfer and with the calculation of the convective flow in the mixing length approximation.

We confirmed the results obtained by [Lesur & Ogilvie \(2010\)](#); [Held & Latter \(2018\)](#) and others that the turbulence generated by convection does not provide the observed rates of disk accretion and sufficient heat influx for which con-

vection would be self-sustaining. There are two reasons for that: the anisotropy of turbulence, as well as the fact that convection is too weak as the source for turbulence.

The first factor manifests itself in the fact that the w_{zz} component of the isotropic part of the Reynolds tensor is excited by convection, while the $w_{r\phi}$ component is responsible for the removal of the angular momentum of the disk. Isotropization of turbulence is not effective enough, which leads to the fact that $w_{r\phi}$ is more than two orders of magnitude smaller than w_{zz} .

To estimate the importance of the second factor, consider the turbulence in the stationary regime near the maximum point of w_{ij} in Fig. 3 or 4 (bottom row, left). Under these conditions, the diffusion term from the equations (60)–(63) disappears and the system of linear algebraic equations with respect to the Reynolds tensor remains, in which the inhomogeneous term has a single non-zero component, B_{zz} . Thus, the solution of the resulting system is proportional to the magnitude of this convective source. In order for the effective accretion rate \dot{M}_{eff} to formally equal the given \dot{M} , it is necessary that the convective flow increase by three orders of magnitude in the ‘A’ model and by four orders of

magnitude in the model ‘B’. This is hardly possible, even taking into account the uncertainty of the mixing length ℓ .

We note that convection can still be an important factor for the problem of angular momentum transfer in a situation where turbulence could be excited not only by convection, but together with instabilities of other types. For example, in the papers of Hirose et al. (2014); Coleman et al. (2018) and Scepi et al. (2018), calculations of 3D MHD models were presented, where it is shown that the joint action of convection and magnetorotational instability can increase α to the observed values.

Of undoubted interest is the study of other hydrodynamic instabilities within the framework of the presented model, such as vertical shear instability, streaming instability, etc. (see the reviews Bae et al. (2022); Lesur et al. (2022)). For example, in the paper Stoll et al. (2017), using numerical simulations, the authors showed that vertical shear instability leads to the appearance of anisotropic turbulence. The review Lesur et al. (2022) also gives examples of other instabilities for which turbulence generation was found in numerical models.

Full-scale 3D simulations allow detailed modeling of nonlinear phenomena in accretion disks. In this case, however, the problem of interpretation arises, i.e. assessment of the significance of one or another physical factor for gas dynamics, transport processes, etc. With this in mind, the model proposed in this paper, being based on the mean field approach and sources, seems to be very useful, since it allows one to explicitly measure the contribution to the dynamics from various factors. At the same time, it should be noted that this approach does not allow one to study the detailed spatial and temporal structure of turbulence, but only its effect on the mean flow.

5 ACKNOWLEDGEMENTS

The authors are grateful to A.V. Tutukov and D.V. Bisikalo for helpful discussions.

The study was supported by a grant from the Russian Science Foundation No. 22-72-10029.

6 DATA AVAILABILITY

Software code and data are available at GITHUB repository via <https://github.com/evgenykurbatov/kp23-turb-conv-ppd>

References

- Andrews S. M., 2020, *ARA&A*, **58**, 483
 Armitage P. J., 2015, arXiv e-prints, p. [arXiv:1509.06382](https://arxiv.org/abs/1509.06382)
 Bae J., Isella A., Zhu Z., Martin R., Okuzumi S., Suriano S., 2022, arXiv e-prints, p. [arXiv:2210.13314](https://arxiv.org/abs/2210.13314)
 Cameron A. G. W., 1978, *Moon and Planets*, **18**, 5
 Canuto V. M., 1992, *ApJ*, **392**, 218
 Canuto V. M., 1993, *ApJ*, **416**, 331
 Canuto V. M., 1997, *ApJ*, **482**, 827
 Coleman M. S. B., Blaes O., Hirose S., Hauschildt P. H., 2018, *ApJ*, **857**, 52
 Flaherty K. M., et al., 2017, *ApJ*, **843**, 150

- Guilloteau S., Dutrey A., Wakelam V., Hersant F., Semenov D., Chapillon E., Henning T., Piétu V., 2012, *A&A*, **548**, A70
 Hansen C. J., Kawaler S. D., 1994, *Stellar Interiors. Physical Principles, Structure, and Evolution..* Springer New York, NY, doi:10.1007/978-1-4419-9110-2
 Harris C. R., et al., 2020, *Nature*, **585**, 357
 Hartmann L., 2009, *Accretion Processes in Star Formation: Second Edition.* Cambridge University Press, Cambridge, UK
 Held L. E., Latter H. N., 2018, *MNRAS*, **480**, 4797
 Held L. E., Latter H. N., 2021, *MNRAS*, **504**, 2940
 Hirose S., Blaes O., Krolik J. H., Coleman M. S. B., Sano T., 2014, *ApJ*, **787**, 1
 Klahr H., 2006, *Proceedings of the International Astronomical Union*, **2**, 405
 Klahr H., Hubbard A., 2014, *ApJ*, **788**, 21
 Lam S. K., Pitrou A., Seibert S., 2015, in *Proceedings of the Second Workshop on the LLVM Compiler Infrastructure in HPC.* pp 1–6
 Landau L. D., Lifshitz E. M., 1959, *Fluid mechanics. Course of theoretical physics*, Oxford: Pergamon Press, 1959
 Launder B., 1974, *Computer Methods in Applied Mechanics and Engineering*, **3**, 269
 Leonard A., 1975, *Advances in Geophysics*, **18**, 237
 Lesur G., Ogilvie G. I., 2010, *MNRAS*, **404**, L64
 Lesur G., et al., 2022, arXiv e-prints, p. [arXiv:2203.09821](https://arxiv.org/abs/2203.09821)
 Lin D. N. C., Papaloizou J., 1980, *MNRAS*, **191**, 37
 Lyra W., 2014, *ApJ*, **789**, 77
 Maksimova L. A., Pavlyuchenkov Y. N., Tutukov A. V., 2020, *Astronomy Reports*, **64**, 815
 Meneveau C., Lund T. S., Cabot W. H., 1996, *Journal of Fluid Mechanics*, **319**, 353
 Nakao Y., Kato S., 1994, *PASJ*, **46**, 273
 Nakao Y., Kato S., 1995, *PASJ*, **47**, 451
 Pavlyuchenkov Y. N., Tutukov A. V., Maksimova L. A., Vorobyov E. I., 2020, *Astronomy Reports*, **64**, 1
 Petzold L., 1983, *SIAM Journal on Scientific and Statistical Computing*, **4**, 136
 Raettig N., Lyra W., Klahr H., 2021, *ApJ*, **913**, 92
 Scepi N., Lesur G., Dubus G., Flock M., 2018, *A&A*, **609**, A77
 Shakura N., ed. 2018, *Accretion Flows in Astrophysics. Astrophysics and Space Science Library Vol. 454*, doi:10.1007/978-3-319-93009-1,
 Shakura N. I., Sunyaev R. A., 1973, *A&A*, **24**, 337
 Speziale C. G., 1991, *Annual Review of Fluid Mechanics*, **23**, 107
 Stewart J. M., 1976, *A&A*, **49**, 39
 Stoll M. H. R., Kley W., Picogna G., 2017, *A&A*, **599**, L6
 Stone J. M., Balbus S. A., 1996, *ApJ*, **464**, 364
 Van Rossum G., Drake F. L., 2009, *Python 3 Reference Manual.* CreateSpace, Scotts Valley, CA, doi:10.5555/1593511
 Virtanen P., et al., 2020, *Nature Methods*, **17**, 261
 Vorobyov E. I., Pavlyuchenkov Y. N., 2017, *A&A*, **606**, A5
 Wogan N., Rackauckas C., 2022, *Nicholaswogan/numbalsoda: numbalsoda v0.3.5*, doi:10.5281/zenodo.7306052, <https://doi.org/10.5281/zenodo.7306052>

This paper has been typeset from a $\text{\TeX}/\text{\LaTeX}$ file prepared by the author.